

# Quantum magnetism in spin-3/2 chains

J. J. Hernández-Sarria<sup>1</sup>, A. Argüelles<sup>1</sup>, K. Rodríguez<sup>1</sup>

E-mail: [karem.c.rodriguez@correounivalle.edu.co](mailto:karem.c.rodriguez@correounivalle.edu.co)

<sup>1</sup>Departamento de Física, Universidad del Valle, AA25360 Cali, Colombia

**Abstract.** Herein, we characterize the quantum phases present in spin-3/2 fermionic chains. This system may be achieved by ultracold gases loaded onto one-dimensional optical lattices in the hard-core regime. The physics of the lowest band in general is described by the Hubbard Hamiltonian that becomes a generalized Heisenberg model in this strongly-correlated regime. By performing calculations of the energy spectrum, correlation functions, level spectroscopy and chirality we analyze the Mott-insulator phases in absence and presence of an external quadratic Zeeman field.

## 1. Introduction

Ultracold gases in optical lattices constitute an extraordinary toolbox for the analysis of strongly-correlated gases under extremely well-controlled conditions [1, 2], as highlighted by the observation of the superfluid to Mott-insulator (MI) transition in ultracold bosons [3], recently followed by the experimental realization of the metal to MI transition in two-component fermions [4, 5]. Optical traps permit simultaneous trapping of various Zeeman sublevels, allowing for multi-component (spinor) formed by atoms with non-zero total spin  $F$ . They constitute an ideal system to investigate the interplay between external and internal (spin) degrees of freedom. As a result of this interplay, the ground state physics is very rich, providing novel scenarios for quantum magnetism. Introducing stronger interactions and smaller occupation number open the fascinating possibility of several insulating phases according to different spin correlations. Manipulation of spins and magnetism has been a motivating goal in a great deal of condensed matter, atom optics and quantum information research. Hence, spinor atoms in optical lattices are good candidates for the achievement of strongly-correlated quantum magnetic systems [6].

Spinor fermions have become the focus of rapidly growing interest, initially motivated by experiments on condensation-superfluidity crossover in two-component fermions [2]. Moreover, the proximity to the Mott insulating phase in fermionic systems is the origin of many intriguing phenomena in condensed matter physics [7]. Such systems are perfect quantum simulators of the Hubbard model and, thus, shed light upon the problem of high  $T_c$  superconductivity. This has been proposed for  $F = 1/2$  [8] and recently considered with three-component fermions [9]. Interestingly, the suppression of conductivity in the system is a result of the interactions and not the consequence of a filled Bloch band like in the usual insulators.

High spin on cold-atomic systems with high symmetries present strong quantum fluctuations [10], rare in condensed matter and worth exploring. Currently, relatively few works have been conducted for high spin fermions, despite their interesting properties.

In this paper, we characterize repulsively interacting spin-3/2 fermions in the Mott-insulator regime. Contrary to spin-1/2, the MI of spin-3/2 presents two distinct magnetic phases



in one dimension (1D) and absence of an external field: a gapless spin liquid (SL) and a gapped dimerized spin Peierls (SP) phase, depending on the inter-atomic interactions. Spin-3/2 fermions are the smallest spin fermionic systems that exhibit spin-changing collisions and, hence, sensitivity to the quadratic Zeeman effect (QZE), or single-ion anisotropy. The QZE role must be taken into account to study high spin systems [11]. Therefore, a detailed analysis with and without an external magnetic field is performed by studying the spectrum, correlations, and level-crossing spectroscopy providing strong numerical proof of the quantum nature of the Mott-phases involved.

## 2. Effective spin-3/2 Hamiltonian with super-exchange interactions

We consider a balanced mixture of spin-3/2 fermions in a 1D lattice with zero total magnetization ( $\mathcal{M} = 0$ ). For a deep lattice and low filling (single-band regime) the most generic Hamiltonian describing 4-component fermions with equal masses interacting via contact potential is given by the Hubbard model. The interaction strengths  $g_{0,2} = 4\pi\hbar^2 a_{0,2}/M$  characterize the  $s$ -wave channels with total spin  $\{0, 2\}$  (the only available due to symmetry), with  $a_{0,2}$  the scattering lengths and  $M$  the atomic mass. Although, typically  $a_0$  and  $a_2$  are similar, their values may be controlled by means of microwave dressing [12] or optical Feshbach resonances [13]. Along this paper, we use the following change of variables (following Ref [11]),  $G = (g_0 + g_2)/2$  and  $g = (g_2 - g_0)/(g_2 + g_0)$ , where  $g$  gives a measurement of the spin-changing collision strength. The interactions preserve  $\mathcal{M}$  and the linear Zeeman effect induced by a magnetic field does not play any role. However, due to spin-changing collisions which re-distribute the populations of the different components while preserving  $\mathcal{M}$ , the QZE becomes crucial in spinor gases. The field is parametrized by the externally tunable constant  $q$  and is experimentally controllable by means of a magnetic field or microwave or optical dressing.

For large-enough interactions and for a chemical potential  $\mu$  larger than a critical value of  $\mu_c(t)$ , the system enters into the MI phase with maximally one fermion per site. Under these conditions, the charge degrees of freedom are frozen and the spin degrees of freedom are described by an effective Hamiltonian with super-exchange interactions, which can be calculated via perturbation theory in the hopping term ( $t$ ). The resulting Hamiltonian is of the form  $\hat{H} = \hat{H}_0 + \hat{H}_{sc}$ , where  $\hat{H}_0$  contains self-energies and spin preserving interactions, whereas  $\hat{H}_{sc}$  has the spin-changing interactions. In the following we will use a renormalized QZE parameter  $\tilde{q}$  defined as  $\tilde{q} = qG/t^2$ .

## 3. Phases in the Mott regime without external fields

When the charge gap opens, the insulating ground state phases are located in the repulsive interaction regime where  $g_{F=0,2} > 0$ . In terms of  $g$  and  $G$ , when  $q = 0$  [14, 15], the ground-state of the system for  $-1 < g \leq 0$  is a gapless spin liquid phase with three gapless spin-modes, including the exactly solvable  $SU(4)$  point ( $g = 0$ ) [16]. For  $0 < g < 1$  the ground state is a spin-Peierls phase, which exhibits a spin gap and long-range dimerization order. At  $g = 0$ , the system undergoes a Kosterlitz-Thouless-like transition between the two phases [17].

*Energy spectrum.* The system energy is plotted as a function of the energy levels in Fig. 1 for several values of the spin-changing strength  $g = \{-0.5, 0, 0.5\}$  and for system size  $L = 6$ . All the main features of the magnetic phases are present in this small system and the results are retrieved by using both full diagonalization and the Lanczos algorithm. One can observe the excited states energies rising with the index level ( $N$ ), following a linear tendency with a non-universal slope in both phases and boundary conditions (BC). For both periodic BC (PBC) panels (a-c) and open BC (OBC) panels (d-f) the decay-rate energy of the spin liquid phase (panels (a-b) and (d-e)) is half smaller than the respective in the dimerized phase (panels (c) and (f)), showing that in the latter this decay is faster including an energy jump given by its characteristic gap.

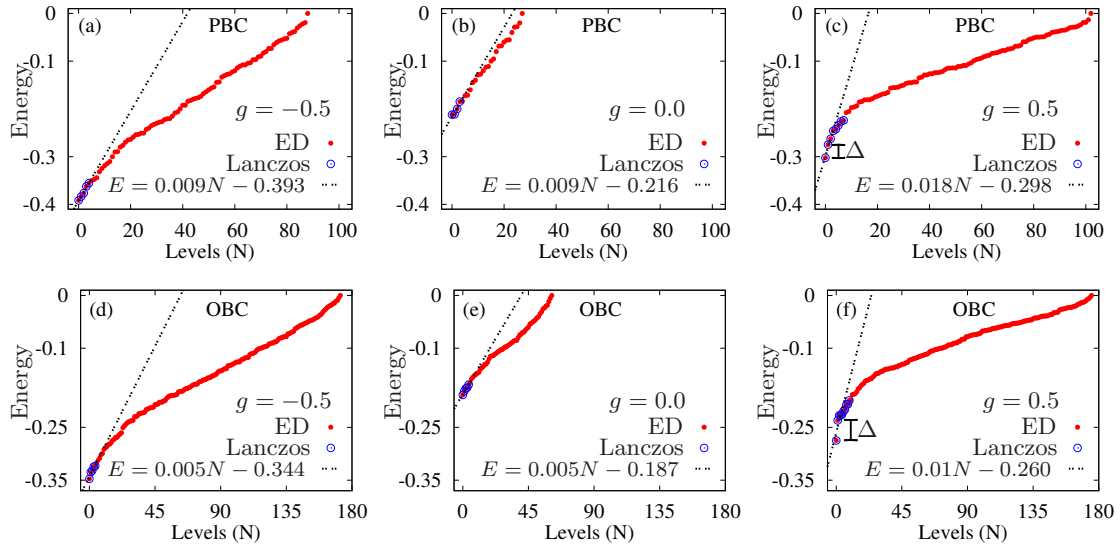


**Figure 1.** Energy spectrum for  $L = 6$  lattice sites without magnetic field for several values of  $g$  using PBC (a) and (b) in the SL phase and (c) in the SP phase. And using OBC (d) and (e) in the SL phase and (f) in the SP phase.

*Energy gap.* The energy gap decays in system size for the dimerized phase. Its behavior is also not universal and depends on the BC. When PBC are imposed, the ground-state is two-fold degenerated in the thermodynamic limit. For OBC, the energy difference is exponentially small in system size. Figure 2 shows that the gap decays exponentially for both periodic (a) and open (b) BC and the values are  $\Delta_{\infty, PBC} = 0.016$  and  $\Delta_{\infty, OBC} = 0.011$ , respectively. Remarkably, the calculations were performed by using the Lanczos algorithm with no more than 10 lattice sites, showing the robustness of this gap.

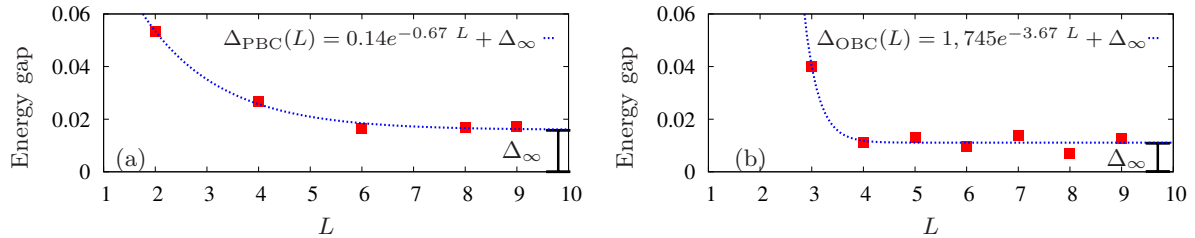


**Figure 2.** Gap-decay in the SP phase using both periodic (a) and open (b) BCs with thermodynamic-limit gap-values  $\Delta_{\infty, PBC} = 0.016$  and  $\Delta_{\infty, OBC} = 0.011$ , using  $g = 0.5$ .

#### 4. Field-induced Mott phases

*Isotropic Heisenberg antiferromagnet (iHAFM) at  $|\tilde{q}| \gg \tilde{q}_c$ .* In the limiting case, for a very strong magnetic field, the degeneracy among  $\pm 1/2$  and  $\pm 3/2$  is lifted, the spin changing superexchange  $H_{sc}$  is negligible, and the two spin manifolds separate. Second-order perturbation theory projects the 4- to a 2-components iHAFM Hamiltonian, favoring one manifold depending on the sign of  $q$  ( $q < 0$  for  $\pm 3/2$  else  $\pm 1/2$ ), see definitions in [11]. Interestingly, the QZE induces phase transitions between the two  $q = 0$  phases and the iHAFM.

*Dimerized phase vs. iHAFM phase ( $g > 0$ ).* In the SP phase, the translational symmetry by one site is spontaneously broken, being a characteristic of 1D systems. In the ground state, neighboring pair of spins with antiferromagnetic interaction tends to form a spin singlet. This arrangement is studied by the dimer-order parameter  $\hat{D}_i = (-1)^i \vec{S}_i (\vec{S}_{i-1} + \vec{S}_{i+1})$  and the long-range order (LRO) in the dimer-dimer correlation (DDC) function  $f_0 = \lim_{\delta \rightarrow \infty} \langle \hat{D}_i \hat{D}_{i+\delta} \rangle$ .

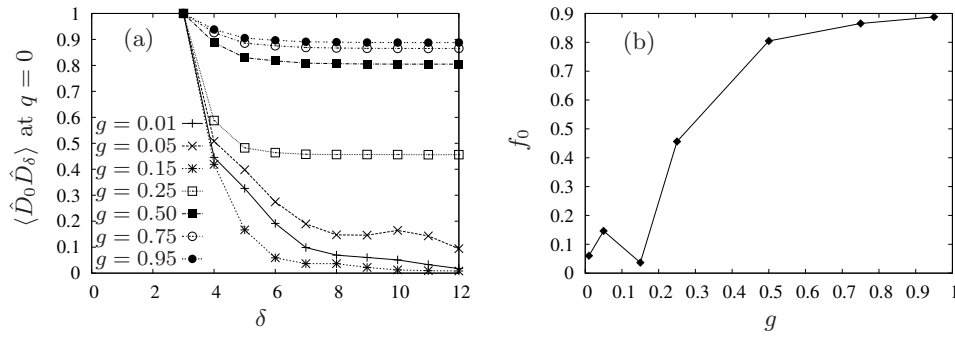


**Figure 3.** (a) DDC spatial function and (b) LRO  $f_0$  as a function of  $g$  at  $q = 0$ .

The calculations were done by using the Density-Matrix Renormalization Group (DMRG) method [18], with up to  $L = 36$ , open BC, and matrix dimension 20. Figure 3 shows a stronger LRO as the interaction  $g > 0$  increases in absence of QZE. In 3(a), the DDC is presented as a function of  $\delta$ , while the panel (b) shows the rise of  $f_0$  with the magnitude of the spin-changing exchange  $g$ .

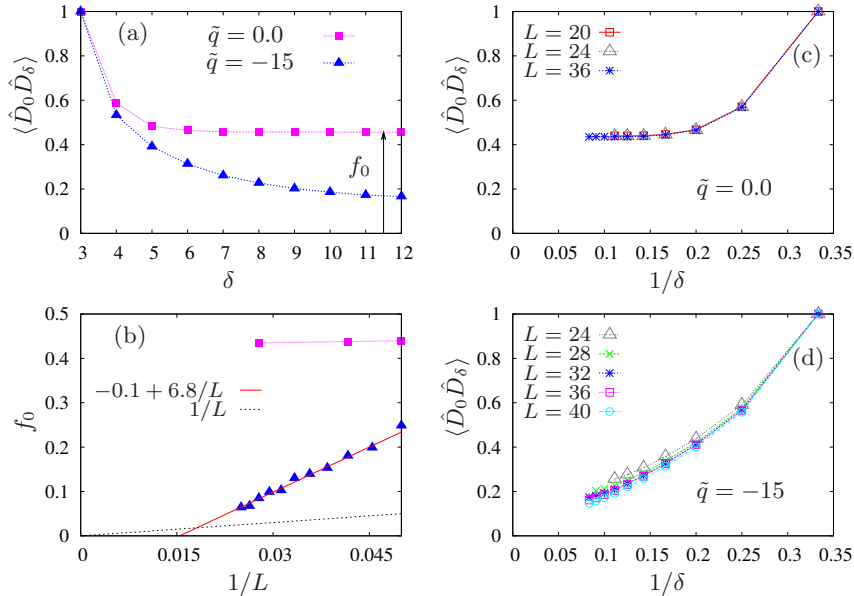


**Figure 4.** (a) DDC for  $\tilde{q} = 0$  and  $\tilde{q} = -15$ . (b) Finite-size scaling  $f_0 \rightarrow 0$  for  $\tilde{q} = -15$  and  $f_0$  is finite for  $\tilde{q} = 0$ . (c) DDC for several system sizes for  $\tilde{q} = 0$  and (d) for  $\tilde{q} = -15$ .

In figure 4(a), we observe that the long-range order disappears in the Heisenberg phase, given that the spatial DDC for  $\tilde{q} = -15$  decays faster compared with the  $q = 0$  case. A finite size scaling has been performed (4(b)), showing the fast decay of  $f_0$  to lower values of  $1/L$  for the iHAFM (filled triangles), while  $f_0$  goes almost constant for the SP (filled squares). Panels (c) and (d) show the DDC as a function of  $1/\delta$ . In (c), the correlation function tends to a finite value for  $q = 0$ , whereas it tends to zero when  $\tilde{q} = -15$  in panel (d). The decay of the spin-spin correlation (SSC) function  $\langle \vec{S}_0 \vec{S}_\delta \rangle$  is shown in Fig. 5(a). The corresponding exponential fit is presented in 5(b) for the SP phase and the algebraic fit is shown in panel (c) for iHAFM, elucidating the 1D counterpart of the 3D Néel order. Panels (d) and (e) present the SSC as a function of  $1/\delta$  for several system sizes, showing fast decay in the dimerized phase at  $q = 0$  and the  $1/\delta$  decay expected for the iHAFM phase.

*Level spectroscopy.* In a finite chain, the two ground states of the dimerized phase split into a unique ground and an excited state separated by an energy gap exponentially small in the

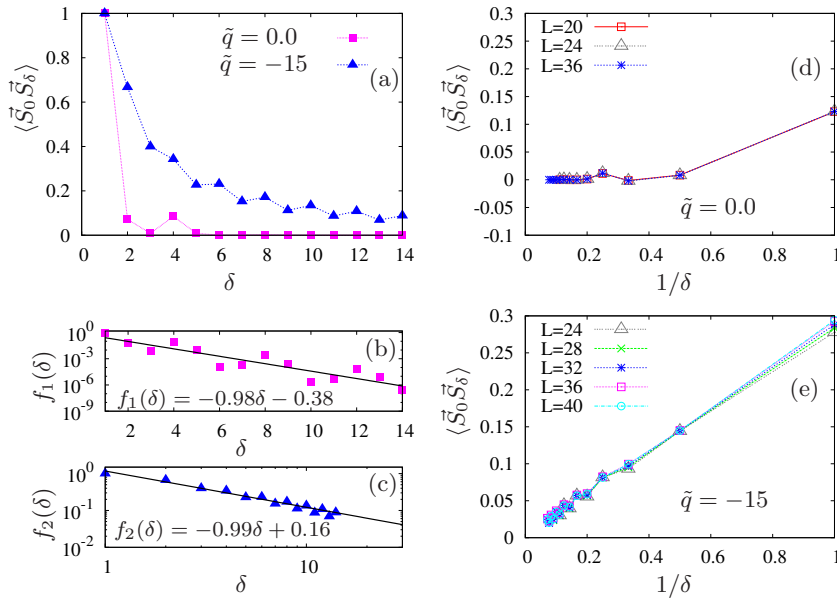


**Figure 5.** (a) SSC for  $\tilde{q} = \{0, -15\}$ . (b) Shows the exponential decay of SSC for  $\tilde{q} = 0$  and (c) the algebraic decay for  $\tilde{q} \gg 1$ . (d) SSC for several system sizes for  $\tilde{q} = 0$  and (e) for  $\tilde{q} = -15$ .

system size for  $0 > |\tilde{q}| > |\tilde{q}_c|$ . In contrast, the lowest excited state in the iHAFM ( $|\tilde{q}| > |\tilde{q}_c|$ ) is a degenerate triplet. Lanczos results show a clear excited singlet-triplet level crossing and the crossing points up to 14 sites with PBC are shown in Fig. 6(a). A finite-size scaling (panel (b)) determines the phase transition line in the thermodynamic limit,  $L_\infty$ , curve in (a), specifying the  $\tilde{q}_c$  values, suggesting a Kosterlitz-Thouless phase transition between the two phases. For large  $g$ , although with non-negligible corrections,  $\tilde{q}_c$  follows a  $1/L^2$  extrapolation like in the  $J_1 - J_2$  AFM chain [19]. For  $g \ll 1$  finite-size effects prevent any reliable extrapolation law.

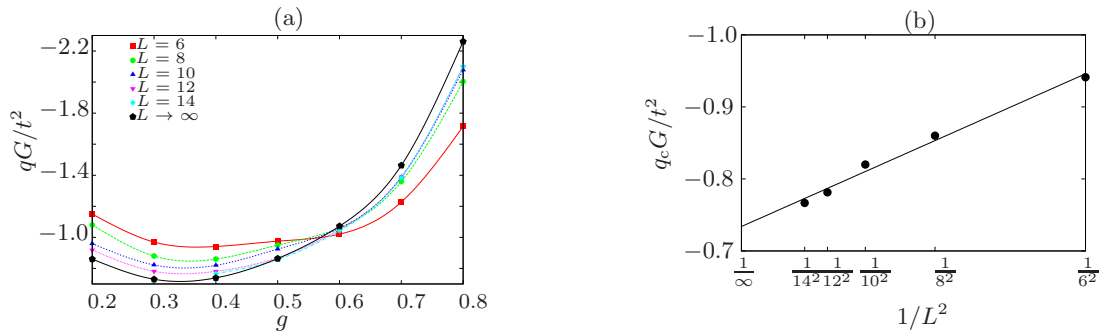


**Figure 6.** (a) Level-crossing spectroscopy for fixing the phase transition boundary for several system sizes. (b) Finite-size scaling example.

*Spin liquid phase vs. iHAFM ( $g \leq 0$ ).* In this case, a phase transition is found between these two gapless phases. Due to the experimental relevance, we monitor in figure 7 (a) the chirality as a function of the QZE,  $\tau = \frac{1}{L}[(N_{3/2} + N_{-3/2}) - (N_{1/2} + N_{-1/2})]$ , ranging from 0 ( $q = 0$ ) to 1 in iHAFM, using the DMRG method.  $\tau$  is conserved only in the absence of the field. On the other hand, the particle number is conserved in each manifold, but the difference between them is not; a fact reflected in the quasi-saturation behavior. The phase transition cannot be identified with  $\tau$  alone, so we study the critical exponent  $\gamma$  of the SSC. Given that, for  $g < 0$  the correlation  $\langle \hat{S}_i^z \hat{S}_j^z \rangle$  oscillates with 4-site periodicity, the bulk correlation envelope function must be studied [20] instead. Thus, we first calculated the bulk SSC function given by  $\langle \hat{S}_i^z \hat{S}_{i+j}^z \rangle_{\text{bulk}} \equiv \frac{1}{4} \sum_{k=0}^3 \langle \hat{S}_{i+k}^z \hat{S}_{i+k+j}^z \rangle$  and later obtained the  $\gamma$  from its envelope decay. This gives

an abrupt jump of  $\gamma$  to  $-1$  at the phase transition (figure 7(b)), preserving the main feature of  $g = 0$  for small enough  $|g|$ . In the iHAFM, the magnetic order is more favorable due to the enhanced antiferromagnetic spin correlations  $\langle \hat{S}_z^i \cdot \hat{S}_z^j \rangle \propto |j - i|^\gamma$  with  $\gamma = -1$ . A jump in  $\gamma$  at  $\tilde{q}_c$  confirms the commensurate-incommensurate nature of the phase transition.  $\gamma$  is relevant only for phases with algebraically decaying correlations, which excludes the SP phase.

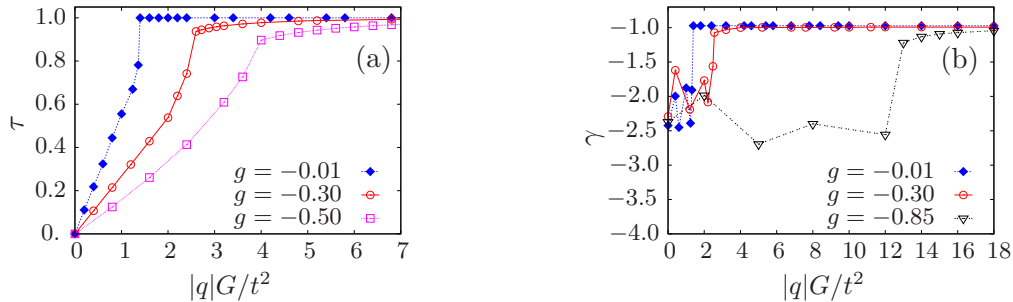


**Figure 7.** (a) Chirality  $\tau$  and (b) critical exponent  $\gamma$  as a function of  $\tilde{q}$  for  $g < 0$ .

## 5. Conclusions

We studied the Mott-insulator phases of spin-3/2 fermions in the absence and presence of an external QZE. We described the pseudo-spin-1/2 iHAFM phase obtained for large enough fields. By decreasing the QZE, this phase undergoes, depending on the scattering lengths, through either a Kosterlitz-Thouless transition into a gapped dimerized phase or a commensurate-incommensurate transition into a gapless spin liquid. In particular, 4-component fermions constitute a unique scenario for experiments on a field-induced commensurate-incommensurate transition. They are the smallest spin fermionic systems that exhibit spin-changing collisions and, hence, sensitivity against QZE.

## Acknowledgments

AA and KR thank Luis Santos and Temo Vekua for their support and fruitful discussions. This work has been partly supported by Universidad del Valle under the project CI-7919. KR thanks the DFG for support (GRK665) and the Center of Excellence for Novel Materials (CENM) at Universidad del Valle for financial support for the research group.

## References

- [1] Lewenstein M, Sanpera A, Ahufinger V, Damski B, Sen A and Sen U 2007 *Advances in Physics* **56** 243–379
- [2] Bloch I, Dalibard J and Zwerger W 2008 *Rev. Mod. Phys.* **80** 885–964
- [3] Greiner M, Mandel O, Esslinger T, Hansch T W and Bloch I 2002 *Nature (London)* **415** 39
- [4] Jördens R, Strohmaier N, Günter K, Moritz H and Esslinger T 2008 *Nature (London)* **455** 204
- [5] Schneider U, Hackermüller L, Will S, Best T, Bloch I, Costi T A, Helmes R W, Rasch D and Rosch A 2008 *Science* **322** 1520–1525
- [6] Jrgensen O, Heinze J and Lhmann D S 2013 *New Journal of Physics* **15** 113017
- [7] Jaramillo J, Greschner S and Vekua T 2013 *Phys. Rev. A* **88**(4) 043616
- [8] Hofstetter W, Cirac J I, Zoller P, Demler E and Lukin M D 2002 *Phys. Rev. Lett.* **89** 220407
- [9] Paananen T, Martikainen J P and Törmä P 2006 *Phys. Rev. A* **73** 053606
- [10] Wang D, Li Y, Cai Z, Zhou Z, Wang Y and Wu C 2014 *Phys. Rev. Lett.* **112**(15) 156403
- [11] Rodríguez K, Argüelles A, Colomé-Tatché M, Vekua T and Santos L 2010 *Phys. Rev. Lett.* **105**(5) 050402
- [12] Papoular D J, Shlyapnikov G V and Dalibard J 2010 *Phys. Rev. A* **81** 041603
- [13] Fedichev P O, Kagan Y, Shlyapnikov G V and Walraven J T M 1996 *Phys. Rev. Lett.* **77** 2913–2916
- [14] Lecheminant P, Boulat E and Azaria P 2005 *Phys. Rev. Lett.* **95** 240402
- [15] Wu C 2005 *Phys. Rev. Lett.* **95** 266404
- [16] Sutherland B 1975 *Phys. Rev. B* **12** 3795–3805
- [17] Wu C 2006 *Mod. Phys. Lett. B* **20** 1707–1738
- [18] Verstraete F and Cirac J I 2006 *Phys. Rev. B* **73** 094423
- [19] Okamoto K and Nomura K 1992 *Physics Letters A* **169** 433 – 437
- [20] Yamashita Y, Shibata N and Ueda K 1998 *Phys. Rev. B* **58** 9114–9118